Characterization of antimicrobial peptide activity by electrochemical impedance spectroscopy

William K. Chang[1], **William C. Wimley**[2], **Peter C. Searson**[1], **Kalina Hristova**[1], and **Mikhail Merzlyakov**[1,*]

1 *Department of Materials Science and Engineering, Johns Hopkins University Baltimore, MD 21218*

2 *Department of Biochemistry, Tulane University Health Science Center New Orleans, LA 70112*

Summary

Electrochemical impedance spectroscopy performed on surface-supported bilayer membranes allows for the monitoring of changes in membrane properties, such as thickness, ion permeability, and homogeneity, after exposure to antimicrobial peptides (AMPs). We show that two model cationic peptides, very similar in sequence but different in activity, induce dramatically different changes in membrane properties as probed by impedance spectroscopy. Moreover, the impedance results excluded the "barrel-stave" and the "toroidal pore" models of AMP mode of action, and are more consistent with the "carpet" and the "detergent" models. The impedance data provide important new insights about the kinetics and the scale of the peptide action which currently are not addressed by the "carpet" and the "detergent" models. The method presented not only provides additional information about the mode of action of a particular AMP, but offers a means of characterizing AMP activity in reproducible, well-defined quantitative terms.

Keywords

Antimicrobial peptides; cationic peptides; electrochemical impedance spectroscopy; planar supported bilayer; membrane electrochemical properties; peptide-membrane interaction

Introduction

Membrane-disrupting peptides and proteins play important biological roles ranging from the innate immune response to the activity of toxins and venoms, and have many potential biotechnological applications in areas including antimicrobial treatment and drug delivery. A detailed understanding of their mechanism of action is crucial. Currently, there are at least four different commonly used models describing possible AMP modes of action: the barrel-stave pore model, the toroidal pore model, the carpet model, and the detergent-like membrane disruption model [1–5]. With the probable exception of the barrel-stave pore model, there is neither agreement on the hypothetical mechanisms described by each model, nor clear distinction between these mechanisms. For example, Shai [1] describes the carpet model as formation of small peptide-lipid aggregates/bicelles, which resembles the detergent model

*corresponding author address: 102 Maryland Hall/3400 N. Charles Street, Baltimore, MD 21218, USA, e-mail: mm1@jhu.edu, phone: 410-516-7142, fax: 410-516-5293.

[2]. Sato and Feix [4] also do not distinguish between the carpet model and the detergent model and comment that in some instances it is difficult to distinguish between carpet and toroidal pore mechanism. In addition, many membrane-active peptides have detergent-like action at high concentrations, independent of their mechanism of action at lower concentrations.

The high-resolution structures of peptides that act according to the barrel-stave model have answered many questions pertaining to their activity [6]. The vast majority of antimicrobial peptides, however, do not follow the barrel-stave model, and questions remain as to which model correctly describes their activity. These questions often specifically focus on explaining the transient nature of peptide induced permeabilization of membrane vesicles [7–12]. This is in part because experimental observations of mechanism are indirect and inconclusive due to the difficulty of following transient processes on a molecular level. Existing experimental methods such as vesicle interaction/leakage assays [7–12] or bacterial sterilization [13–17] are limited to properties of the whole ensemble of peptides. Structural measurements [18–20] are often performed after peptide-membrane interaction and membrane permeabilization has already taken place, instead of during the transient processes. Although all of these methods yield valuable information about peptide activity, they provide an incomplete picture of the detailed mechanism of AMP mode of action. The purpose of this work is to use electrochemical impedance spectroscopy (EIS) as a new experimental approach to study AMP interaction with membranes in order to obtain additional and complimentary information to AMP activity studies and to address the controversy surrounding the mechanism of action of antimicrobial peptides. EIS [21] monitors the integrity of lipid membranes in real time and is very sensitive to changes in membrane properties such as membrane thickness, membrane heterogeneity and ion permeation. We use a lipid bilayer with a polyethylene glycol cushion supported on a silicon substrate as a biomimetic platform on which the activity of AMPs can be monitored by measuring changes in the bilayer impedance. Surface-supported bilayers have been shown to preserve lateral mobility of lipids and proteins in the bilayer, which is essential for the biomimetic properties and the incorporation of many membrane proteins and peptides [22]. Bilayer membranes formed by Langmuir-Blodgett (LB) deposition on single crystal silicon have been shown to be excellent electrochemical models of cell membranes [23]. In addition, this biomimetic platform allows control over the composition of the lipids in the bilayer as well as over the membrane potential. The latter feature allows modulation of the activity of AMPs, but it is difficult to maintain a non-zero membrane potential when measurements are carried out in liposomes. Here we measured the effect of two antimicrobial peptides, selected from a combinatorial library [24], on bilayer impedance. These antimicrobial peptides have very similar sequences but show very different activity in vesicle leakage assays [25], therefore they are particularly interesting for demonstrating the feasibility and the sensitivity of the proposed approach to study AMP activity. The results of EIS are compared with the expected activity and are consistent with vesicle leakage assays. The results can be interpreted within the framework of existing models of AMP mode of action. In addition, EIS can reveal important new details about AMP activity that are not accessible by other experimental techniques, thus advancing the research in the field of antimicrobial peptides.

Materials and Methods

Peptides

Two cationic peptides, each 26 residues long and sequentially identical except for five combinatorially variable sites at positions 4, 5, 7, 20 and 23, were chosen from a library [24]. The peptides exhibit similar antimicrobial activity but act differently in vesicle leakage assay [25], therefore one is named a potent pore-former and the other is a poor pore-former. The sequence of the potent pore-former is RRG**FS**L**K**LALAKDGWALML**R**LG**Y**GRR (original library designation **FSKRGY** [24]), and the sequence of the poor pore-former is

RRG**AG**L**G**LALAKDGWALML**K**LG**F**GRR (**AGGK**GF). The peptides were synthesized and purified by solid phase synthesis and high-performance liquid chromatography, respectively [25].

Substrate

N-type silicon (111) wafers (Silicon Quest International, Inc., Santa Clara, CA) with a thickness of 425–475 μm and a resistivity of 0.001–0.005 Ωcm were used for all experiments. The wafers were cleaned by sequential immersion in 2-propanol (Fisher Scientific), acetone (Pharmaco-Aaper), and 2-propanol, sonicating for 10 minutes in each solvent, and stored in DI water at room temperature. Each wafer was individually cleaned for 30 minutes in a fresh mixture of 30% hydrogen peroxide (Fisher Scientific) and 70% sulfuric acid (Fisher Scientific) and rinsing 10 times with DI water.

Bilayer formation

Lipid bilayers were formed on the silicon wafers by first depositing Langmuir-Blodgett (LB) monolayer using a Langmuir trough (Model 611D, Nima Technology Ltd., Coventry, England), followed by vesicle fusion. 1,2-diphytanoyl-sn-glycerol-3-phosphocholine (DPhPC) and 1,2-dipalmitoyl-sn-glycero-3-phosphoethanolamine-N-[methoxy(polyethylene glycol)-2000] (PEG2k) were purchased from Avanti Polar Lipids and used without further purification. DPhPC provides high membrane resistance while retaining membrane fluidity, and is therefore often used as the main lipid component in EIS experiments [26,27]. Previous EIS characterization of melittin and gramicidin [27] has utilized DPhPC, such that these results can be directly compared with the results presented in the current study. DPhPC and PEG2k were mixed at the crossover concentration [28], 94.1% to 5.9%, in chloroform (Fisher Scientific) for a total lipid concentration of 1mg/ml. For vesicle preparation, DPhPC lipids dried from chloroform were rehydrated with buffer (pH = 7, 100 mM NaCl, 10 mM phosphate) for a final lipid concentration of 1 mg/ml. The lipid suspension was extruded ten times using a mini-extruder (Avanti Polar Lipids, Alabaster, AL) through a polycarbonate membrane with a pore diameter of 100 nm (Whatman).

For each LB deposition, the silicon substrate was attached to the dipping mechanism of the trough and lowered into the subphase, 18 MΩ cm water (Millipore, Bedford, MA). 20 μl of the chloroform lipid solution was spread dropwise on the water surface of the open trough (600 cm^2), and the solvent was allowed to evaporate for 15 minutes. The monolayer was then compressed at a speed of 100 cm^2/min to a target pressure of 42 mN/m, and the substrate was raised at 15 mm/min while maintaining the target pressure.

The substrate, supporting the monolayer, was assembled into an electrochemical half-cell. A small area of the oxide layer was removed from the surface of the substrate outside the cell by carefully applying 25% hydrofluoric acid with a cotton swab and a contact point was made with gallium-indium eutectic. The electrochemical cell was filled with 5ml buffer (pH = 7, 100 mM KCl, 10 mM phosphate). The total area of the bilayer in contact with the buffer was 0.8 cm^2. Ag/AgCl (3 M KCl) reference electrode was connected to the cell via a Luggin capillary.

The electrodes were connected to a computer-controlled lock-in amplifier (DSP-7265, Ametek, TN). A DC bias of 0 V was forced and impedance spectrum measurements were started. Measurements were taken at an AC perturbation of 20 mV with DC bias potentials 0 V, 0.5 V, and 1.0 V of Ag/AgCl, over the frequency range from 1 to 10^5 Hz, with each scan lasting ~1 min. After the first scan was completed, 100 μl of vesicle solution was added using a gel-loading pipette tip inserted through the hole in the platinum mesh counter-electrode, ~2 mm beneath the platinum mesh. Change of electrochemical impedance with time during vesicle fusion was observed and found to reach equilibrium after ~25 minutes. Vesicle fusion was

allowed to proceed for 40 minutes before adding peptides. For experiments at positive DC bias, the bias was changed from 0 V to the desired potential and the system was allowed to re-equilibrate for another 20 minutes prior to adding peptides.

Peptide delivery

Both FSKRGY and AGGKGF were delivered in 0.1% acetic acid stock solution with a peptide concentration ~12 μM, which was determined using tryptophan and tyrosine absorbance. The peptide solutions were then added to the electrochemical cell via a gel-loading pipette inserted ~2 mm under the counter-electrode, using different volumes to achieve desired peptide/lipid ratios. Previous high-throughput screening assays [24,25] had determined 1/500 P/L as the lowest concentration with observed pore-formation, and this was used as the minimum peptide concentration for experiments. Peptide/lipid ratios were taken as the ratio between the number of peptide molecules and the number of total lipid molecules in the electrochemical cell, present in both the tethered bilayer and in the free unfused vesicles in the buffer. Experiments were also performed where free vesicles were removed from the electrochemical cell by repeated removal and replacement of the buffer.

Impedance measurements continued for 25 minutes after adding the peptides. The addition of 0.1% acetic acid without peptides (in negative control experiments) did not induce any detectable changes in the impedance spectra.

Data analysis

The impedance data were analyzed using the complex nonlinear least-squares immittance fitting program (Zview, Scribner Associates). The substrate-bilayer-buffer system was modeled as an equivalent circuit with a resistor in series with a resistor-capacitor pair and a resistor-constant phase element pair (see Fig. 1). Three components were used for further analysis: the bilayer resistance R_m, the capacitance term Q, and the exponent term n of the constant phase element (CPE) (see the Theory section below).

Theory

A bilayer membrane in a moderate electrical field can be modeled as a capacitor in parallel with a resistance. For an ideal membrane there is no ion transport across the bilayer (infinite resistance) and the membrane behaves like a dielectric medium with charge build up on either side. Finite membrane resistance determines the rate of ion diffusion through the bilayer. AMPs interacting with the membrane affect both capacitance and resistance values. For example, membrane thinning caused by AMPs would lead to an increase in the membrane capacitance, which is given (per unit area) as:

$$C_m = \varepsilon/d, \tag{1}$$

where ε and d are the permittivity and membrane thickness, respectively. Similarly, ion channels or defects formed by AMPs would lead to a decrease in the membrane resistance. The capacitance and the resistance of the membrane can be directly measured by EIS, thus revealing the effects of AMPs on the membrane. To allow quantitative analysis of the membrane homogeneity we use a constant phase element (CPE) as a more general representation of membrane capacitance. The impedance of a CPE as a function of angular frequency ω is given by

$$Z_{CPE}(\omega) = \frac{1}{Q(i\omega)^n} \tag{2}$$

where n is a measure of membrane homogeneity: the lower the n value, the more heterogeneous the membrane is. When $n = 1$, the membrane is homogeneous and Q is equivalent to the membrane capacitance. When $n \neq 1$, the membrane capacitance can be estimated as

$$C_m(\omega) = Q \cdot \omega^{n-1}$$

(3)

and is frequency dependent; for $n < 1$, C_m is higher at lower frequency. This can be explained by the fact that thinner membrane regions (regions with higher capacitance) have lower time constants and therefore contribute more at low frequencies while membrane thickest regions contribute at highest frequency.

Thus there are at least three electrical parameters describing the membrane: (i) the membrane resistance R_m as a measure of membrane "leakiness", i.e. the degree of lipid order and the presence of ion channels or membrane defects, (ii) the exponent n as a measure of membrane homogeneity, (iii) the membrane capacitance C_m as a measure of membrane thickness. Fig. 2 shows four different AMP modes of action [1–5] and anticipated electrochemical response.

Results

The impedance spectra of a DPhPC/PEG2k bilayer before and after exposure to AGGKGF at a 1/100 P/L ratio are shown in Fig. 3. Prior to peptide injection, the membrane is fairly homogeneous and can be described by ideal capacitance C_m and resistance R_m, as shown in Fig. 3 (top panel); it is the action of AMPs which, depending on the mode of action, render the membrane heterogeneous and lead to changes in membrane thickness and "leakiness". The use of the equivalent circuit shown in Fig. 1 results in a good fit to the measured impedance. Such impedance spectra were taken every minute and the values for R_m, n and Q, along with uncertainties from the fit, were determined for each spectrum.

Fig. 4 shows the membrane resistance versus time before and after exposure to the peptides. The addition of either FSKRGY or AGGKGF induces a significant decrease in membrane resistance within one minute of exposure to the bilayer. The final value for the membrane resistance R_m in the presence of FSKRGY is ~1 kΩ cm^2, while R_m ~ 5 kΩ cm^2 in the presence of AGGKGF, a five fold difference. This shows that the potent pore-former FSKRGY causes greater permeability of in the membrane than the poor pore-former AGGKGF.

The effect of peptide addition on membrane homogeneity is qualitatively different from the changes in membrane resistance: while FSKRGY induces heterogeneity in the membrane with the exponent n reaching minimum values of 0.70~0.79 depending on bias, the addition of AGGKGF causes no measurable effect on membrane homogeneity (see Fig. 5). In the experiments with FSKRGY, more positive membrane potentials result in less significant changes. In addition, the changes are smaller at lower peptide concentration. Values of n reach minima within 1–2 minutes, followed by partial relaxation (recovery) with a time constant of about 8 minutes.

Experiments were also performed where free vesicles were removed from the electrochemical cell by repeated removal and replacement of the buffer. Results from these experiments (not shown) were similar to experiments with free vesicles present in the buffer, but changes in homogeneity and its recovery were less pronounced. Note that we used ~10 times less peptides to keep the same peptide/lipid ratio in vesicle-free experiments; therefore final bulk peptide concentration was much lower. Lower bulk concentration would result in lower peptide partitioning into the supported membrane and to weaker overall effect.

As mentioned in the Theory section, the capacitance of a heterogeneous membrane is frequency dependent. At 5 kHz, close to the highest frequency at which C_m contributes to the measured

impedance, the membrane capacitance remains the same ($C_m = 0.87$ μF/cm^2) before and after exposure to the peptides, even when the membrane impedance exhibits large changes. This result demonstrates that in all experiments the membrane thickness remains the same in some regions while in other regions its thickness decreases when membrane homogeneity decreases.

Discussion

The presented EIS data allow us to evaluate the range of possible AMP modes of action. We have previously shown that channel-forming peptides, such as gramicidin, change only membrane resistance in a concentration-dependent fashion and do not change the homogeneity and the capacitance of a surface-supported membrane [23]. Purrucker *et al* have shown that channel-forming peptides do not change homogeneity of a surface-supported membrane [30]. Similarly, addition of melittin, which acts according to the barrel-stave model, to the bilayer leads to two orders of magnitude drop in membrane resistance, while membrane capacitance and homogeneity remain practically the same [27]. In contrast, we observed a large decrease in membrane homogeneity in the presence of the potent pore-former FSKRGY. Moreover, membrane resistance is not dependent on peptide concentration within the range tested for both the potent and poor pore-formers. Therefore, these AMPs do not act according to the barrel-stave model.

For a toroidal pore model it is expected that the pore density increases (lower membrane resistance) with higher peptide concentration. No such trend was observed for both peptides. In addition, the observed recovery of membrane homogeneity is not expected for the toroidal pore model. If the toroidal pore acts like a gate for the peptides to translocate to the other side of the membrane, the pores themselves should be transient and disintegrate with time as the concentration of the peptides on both sides of the membrane equilibrates. The pore disintegration should lead to an increase in membrane resistance, which was not observed.

According to the carpet model, peptides aggregate upon binding to the bilayer, thus decreasing bilayer homogeneity and possibly decreasing bilayer resistance. Therefore, the carpet model is consistent with our experimental observations. However, the observed recovery in membrane homogeneity in experiments with FSKRGY is somewhat unexpected. After an initial minimum is reached, a recovery to a more homogeneous membrane is always observed in EIS experiments. It is therefore possible that carpet "rafts" form within the first minute, and that the observed recovery occurs after membrane destabilization by the lateral redistribution of lipids/peptides. Since the carpet model does not explicitly describe how and why rafts destabilize the membrane, we cannot definitively rule out or support this model using the impedance data. Nonetheless, we can conclude that aggregation and membrane destabilization should occur within the first minute of the membrane exposure to the peptides, and that such destabilization should be localized, since the overall membrane remains intact and still exhibits a measurable resistance.

The observed decrease in homogeneity and membrane resistance in FSKRGY experiments is also expected from the detergent model. However, since the membrane remains intact and still exhibits measurable resistance, the membrane disruption/dissolution occurs locally and is consequently repaired by the lateral diffusion of lipids into the damaged area, and there is no large scale membrane disruption. Note that "healing" the disrupted regions by vesicle fusion should inevitably decrease the ion permeability (increase the membrane resistance), which was not observed. Therefore we have to rule out the fusion of free vesicles as a possible recovery mechanism. Thus the reparative behavior should be incorporated into the detergent model to explain the observed recovery of membrane homogeneity.

There is another important consideration for both the carpet and the detergent models. The constant value of the membrane capacitance C_m at high frequency together with the observed decrease in homogeneity implies that the membrane thickness stays the same in some regions and gets thinner in the other regions after peptide interactions. Since membrane thinning is expected upon interaction with AMP (see eg. [31]), these local regions of decreased thickness are most likely the sites of peptide interactions. The observed partial recovery towards a more homogeneous membrane implies that, with time, the thinned regions do equilibrate to some extent with the rest of the membrane. This recovery is reminiscent of the recovery in vesicle leakage assays: the rate of efflux becomes smaller, with a time constant of a few minutes [9].

AGGKGF does not induce leakage in high-stringent assays (1/500 P/L) while FSKRGY does [25] and both peptides exhibit anti-microbial activity by sterilizing bacterial cultures at concentrations of ~2 μM whereas only AGGKGF had significant cytotoxicity and hemolytic activity against human cells [25].

We found that both peptides reduce membrane resistance, which may be correlated with antimicrobial activity. There are changes in membrane resistance even at high stringency, under conditions where AGGKGF should be inactive according to the vesicle leakage assay. The reason for the observed AGGKGF activity at high stringency might be the fact that EIS is sensitive to any ions that can leak through the membrane, while the leakage assay detects the leakage of particular encapsulated molecules. Thus EIS may be more sensitive than the vesicle leakage assays to the membrane effects that are important in antimicrobial activity. Note that some AMPs, like dermaseptins, cecropin B, cecropin P and cecropin A dissipate ion gradients at low peptide concentration, while much higher concentrations are required to release encapsulated fluorescent probe [32,33]. It is possible that AGGKGF acts in a similar manner, which can explain the potent sterilization activity of AGGKGF (via dissipation of ion gradient) despite the poor vesicle leakage activity. AGGKGF may merely adhere/intercalate into the membrane and cause lipid local disordering leading to some ion leakage, thus decreasing membrane resistance. FSKRGY peptides, in addition to the above-mentioned lipid disordering, aggregate and disrupt the membrane, thus further decreasing the membrane resistance. FSKRGY aggregates more strongly at higher concentration (lower n at 1/100 P/L than at 1/500 P/L), as expected. In contrast to FSKRGY, there is no change in homogeneity upon addition of AGGKGF. This difference in peptide behavior correlates with lytic activity in vesicles: AGGKGF does not cause vesicle leakage at high stringency, whereas FSKRGY does. This suggests that lytic activity is a consequence of peptide aggregation and of increase in membrane heterogeneity.

It is well known that the activity of AMPs strongly depends on the presence of negatively charged lipids in the target membrane. The bias potential effectively sets the charge density of the tethered membrane by means of ion accumulation on the membrane surface, thus modulating the peptide partitioning into the membrane. Membrane potentials affect the partitioning of peptides into membranes [34], as well as the orientation and the degree of penetration of the peptides within the membranes [35], consistent with our results. We observed that the aggregation of FSKRGY depends on the membrane potential: change in membrane potential from zero to a positive bias reduced aggregation. Thus, the membrane potential is an additional parameter that can be used to characterize and to modulate peptide activity. In general, EIS on a surface-supported bilayer offers the unique possibility to vary and maintain the membrane potential during peptide-membrane interactions, which is often impossible to do in other assays.

The results reported here illustrate the general requirements for studying AMP-membrane interaction using EIS. First, the surface-supported membrane should be spatially homogeneous, that is the lipids should form a continuous single phase without rafts. Second, the membrane

should be in the fluid phase to provide lateral mobility of membrane-associated peptides. Third, the membrane should be decoupled from the solid support via a polymer cushion or spacer in order to better accommodate possible peptide-induced lateral stress or local membrane curvature. Finally, the ion permeability of the membrane should be low to maximize the range for detection of AMP interactions. Low ion permeability can be achieved when lipids are densely packed and well ordered; the addition of cholesterol to low-density disordered lipids can improve membrane resistance.

Conclusions

Using impedance spectroscopy, we characterized the mode of action of two AMPs, a pore-former and a non pore former [24,25]. Our observations of the electrochemical response of membranes in the presence of these AMPs support the carpet or detergent model for AMP mode of action with the new findings: (i) membrane destabilization occurs within the first minute of membrane exposure to AMPs; (ii) disruption/dissolution of the membrane occurs locally and is consequently repaired, without leaving large patches of dissolved membrane; (iii) recovery occurs after membrane destabilization, either by the re-equilibration of lipids/ peptides to achieve a more even distribution (within the framework of the carpet model), or by lipid lateral diffusion from the intact regions into the dissolved flaws (within the framework of the detergent model); (iv) after exposure to the peptides, the membrane thickness in some regions remains the same, in other regions (the sites of peptide interactions) it is reduced.

We have confirmed that FSKRGY has significantly more potent membrane-disrupting activity than AGGKGF, supporting results of previous vesicle leakage assay [25]. On the other hand, both peptides increase the ion permeability of the membrane, supporting the results of bacterial sterilization assay [25]. Positive membrane potentials decrease FSKRGY ability to aggregate and to disrupt the membrane, which is consistent with the notion that negative membrane charges are important for AMP activity.

We have demonstrated that EIS can be used to characterize and differentiate the activity of AMPs. This approach can be utilized to study the influence of any antimicrobial peptide on membrane ion permeability and heterogeneity. This information can, in turn, be used to distinguish peptides by their modes of action and to assess their potency in membrane destabilization.

Acknowledgements

References

1. Shai Y. Mode of action of membrane active antimicrobial peptides. Biopolymers 2002;66:236–248. [PubMed: 12491537]

2. Bechinger B. Structure and function of membrane-lytic peptides. Critical Reviews in Plant Sciences 2004;23:271–292.

3. Brogden KA. Antimicrobial peptides: Pore formers or metabolic inhibitors in bacteria? Nature Reviews Microbiology 2005;3:238–250.

4. Sato H, Feix JB. Peptide-membrane interactions and mechanisms of membrane destruction by amphipathic alpha-helical antimicrobial peptides. Biochimica et Biophysica Acta 2006;1758:1245–1256. [PubMed: 16697975]

5. Hoskin DW, Ramamoorthy A. Studies on anticancer activities of antimicrobial peptides. Biochimica et Biophysica Acta 2008;1778:357–375. [PubMed: 18078805]

6. Porcelli F, Buck B, Lee DK, Hallock KJ, Ramamoorthy A, Veglia G. Structure and orientation of pardaxin determined by NMR experiments in model membranes. J Biol Chem 2004;279:45815–45823. [PubMed: 15292173]

7. Wimley WC, Selsted ME, White SH. Interactions between human defensins and lipid bilayers – evidence for formation of multimeric pores. Protein Science 1994;3:1362–1373. [PubMed: 7833799]

8. Ladokhin AS, Wimley WC, Hristova K, White SH. Mechanism of leakage of contents of membrane vesicles determined by fluorescence requenching. Methods in Enzymology 1997;278:474–486. [PubMed: 9170328]

9. Chen HM, Clayton AHA, Wang W, Sawyer WH. Kinetics of membrane lysis by custom lytic peptides and peptide orientations in membrane. Eur J Biochem 2001;268:1659–1669. [PubMed: 11248685]

10. Matsuzaki K, Murase O, Miyajima K. Kinetics of pore formation by an antimicrobial peptide, magainin-2, in phospholipid-bilayers. Biochemistry 1995;34:12553–12559. [PubMed: 7548003]

11. Matsuzaki K, Murase O, Fujii N, Miyajima K. Translocation of a channel-forming antimicrobial peptide, magainin-2, across lipid bilayers by forming a pore. Biochemistry 1995;34:6521–6526. [PubMed: 7538786]

12. Pokorny A, Almeida PFF. Kinetics of dye efflux and lipid flip-flop induced by delta-lysin in phosphatidylcholine vesicles and the mechanism of graded release by amphipathic, alpha-helical peptides. Biochemistry 2004;43:8846–8857. [PubMed: 15236593]

13. Haukland HH, Ulvatne H, Sandvik K, Vorland LH. The antimicrobial peptides lactoferricin B and magainin 2 cross over the bacterial cytoplasmic membrane and reside in the cytoplasm. FEBS Lett 2001;508:389–393. [PubMed: 11728458]

14. Vogt TCB, Bechinger B. The interactions of histidine-containing amphipathic helical peptide antibiotics with lipid bilayers - The effects of charges and pH. J Biol Chem 1999;274:29115–29121. [PubMed: 10506166]

15. Chan SC, Yau WL, Wang W, Smith DK, Sheu FS, Chen HM. Microscopic observations of the different morphological changes caused by anti-bacterial peptides on Klebsiella pneumoniae and HL-60 leukemia cells. J Peptide Sci 1998;4:413–425. [PubMed: 9851369]

16. Matsuzaki K, Sugishita K, Harada M, Fujii N, Miyajima K. Interactions of an antimicrobial peptide, magainin 2, with outer and inner membranes of Gram-negative bacteria. Biochim Biophys Acta 1997;1327:119–130. [PubMed: 9247173]

17. Oren Z, Shai Y. Cyclization of a cytolytic amphipathic alpha-helical peptide and its diastereomer: Effect on structure, interaction with model membranes, and biological function. Biochemistry 2000;39:6103–6114. [PubMed: 10821683]

18. Lee MT, Chen FY, Huang HW. Energetics of pore formation induced by membrane active peptides. Biochemistry 2004;43:3590–3599. [PubMed: 15035629]

19. Yang L, Harroun TA, Weiss TM, Ding L, Huang HW. Barrel-stave model or toroidal model? A case study on melittin pores. Biophys J 2001;81:1475–1485. [PubMed: 11509361]

20. Henzler-Wildman KA, Lee DK, Ramamoorthy A. Mechanism of lipid bilayer disruption by the human antimicrobial peptide, LL-37. Biochemistry 2003;42:6545–6558. [PubMed: 12767238]

21. Macdonald, JR. Impedance Spectroscopy Emphasizing Solid Materials & Systems. John Wiley & Sons; New York: 1987.

22. Merzlyakov M, Li E, Hristova K. Directed assembly of surface-supported bilayers with transmembrane helices. Langmuir 2006;22:1247–1253. [PubMed: 16430290]

23. Nikolov V, Lin J, Merzlyakov M, Hristova K, Searson PC. Electrical measurements of bilayer membranes formed by Langmuir-Blodgett deposition on single-crystal silicon. Langmuir 2007;23:13040–13045. [PubMed: 18004893]

24. Rausch JM, Marks JR, Wimley WC. Rational combinatorial design of pore-forming beta-sheet peptides. Proc Natl Acad Sci USA 2005;102:10511–10515. [PubMed: 16020534]

25. Rausch JM, Marks JR, Rathinakumar R, Wimley WC. beta-Sheet pore-forming peptides selected from a rational combinatorial library: Mechanism of pore formation in lipid vesicles and activity in biological membranes. Biochemistry 2007;46:12124–12139. [PubMed: 17918962]

26. Atanasov V, Knorr N, Duran RS, Ingebrandt S, Offenhäusser A, Knoll W, Köper I. Membrane on a chip: a functional tethered lipid bilayer membrane on silicon oxide surface. Biophys J 2005;89:1780–1788. [PubMed: 16127170]

27. He LH, Robertson JWF, Li J, Kärcher I, Schiller SM, Knoll W, Naumann R. Tethered bilayer lipid membranes based on monolayers of thiolipids mixed with a complementary dilution molecule. 1. Incorporation of channel peptides. Langmuir 2005;21:11666–11672. [PubMed: 16316098]

28. Merzlyakov M, Li E, Gitsov I, Hristova K. Surface-supported bilayers with transmembrane proteins: Role of the polymer cushion revisited. Langmuir 2006;22:10145–10151. [PubMed: 17107013]

29. Marsh D, Pali T. The protein-lipid interface: perspectives from magnetic resonance and crystal structures. Biochim Biophys Acta 2004;1666:118–141. [PubMed: 15519312]

30. Purrucker O, Hillebrandt H, Adlkofer K, Tanaka M. Deposition of highly resistive lipid bilayer on silicon-silicon dioxide electrode and incorporation of gramicidin studied by ac impedance spectroscopy. Electrochimica Acta 2001;47:791–798.

31. Heller WT, Waring AJ, Lehrer RI, Harroun TA, Weiss TM, Yang L, Huang HW. Membrane thinning effect of the beta-sheet antimicrobial protegrin. Biochemistry 2000;39:139–145. [PubMed: 10625488]

32. Gazit E, Boman A, Boman HG, Shai Y. Interaction of the mammalian antibacterial peptide cecropin p1 with phospholipid-vesicles. Biochemistry 1995;34:11479–11488. [PubMed: 7547876]

33. Silvestro L, Gupta K, Weiser JN, Axelsen PH. The concentration-dependent membrane activity of cecropin A. Biochemistry 1997;36:11452–11460. [PubMed: 9298965]

34. Stankowski S, Schwarz UD, Schwarz G. Voltage-dependent pore activity of the peptide alamethicin correlated with incorporation in the membrane: salt and cholesterol effects. Biochim Biophys Acta 1988;941:11–18. [PubMed: 2453215]

35. Sansom MS. Alamethicin and related peptaibols – model ion channels. Eur Biophys J 1993;22:105–124. [PubMed: 7689461]
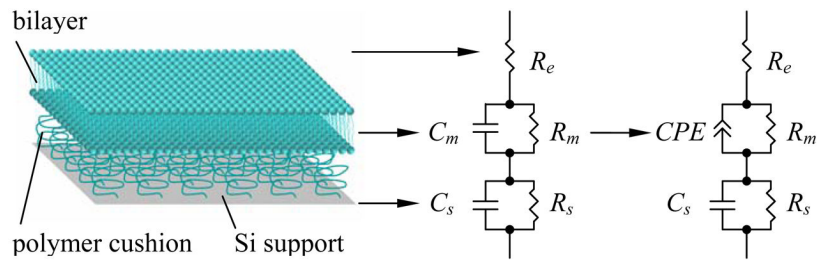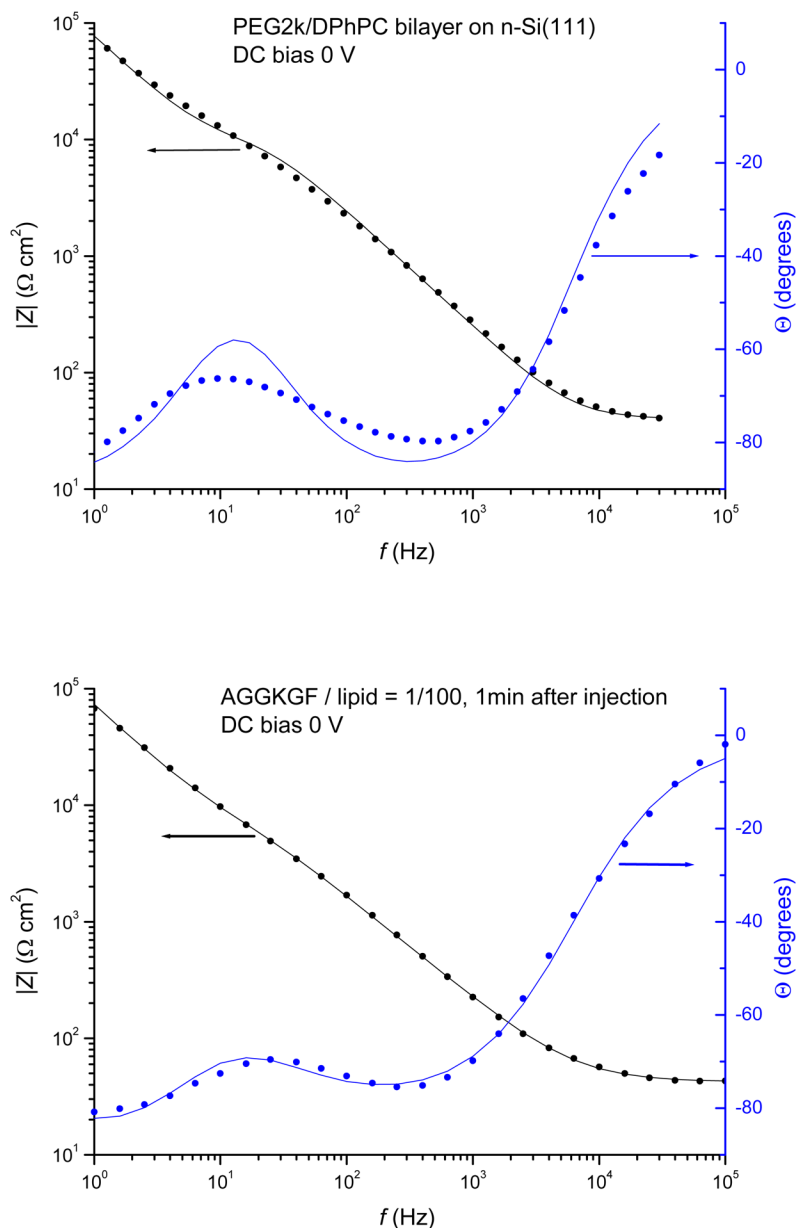
Figure 1.
A surface-supported bilayer and its equivalent electrical circuit. The R_sC_s element corresponds to the support-electrolyte interface with the resistance R_s describing solid-to-liquid charge transfer due to redox reaction and C_s being the double layer and the space charge capacitance, while the R_mC_m (or R_mCPE) element corresponds to the resistance and capacitance of the bilayer, and the series resistor R_e corresponds to the resistance of the electrolyte (buffer). The values of all electrical components are experimentally determined by measuring electrochemical impedance of the surface-supported bilayer.
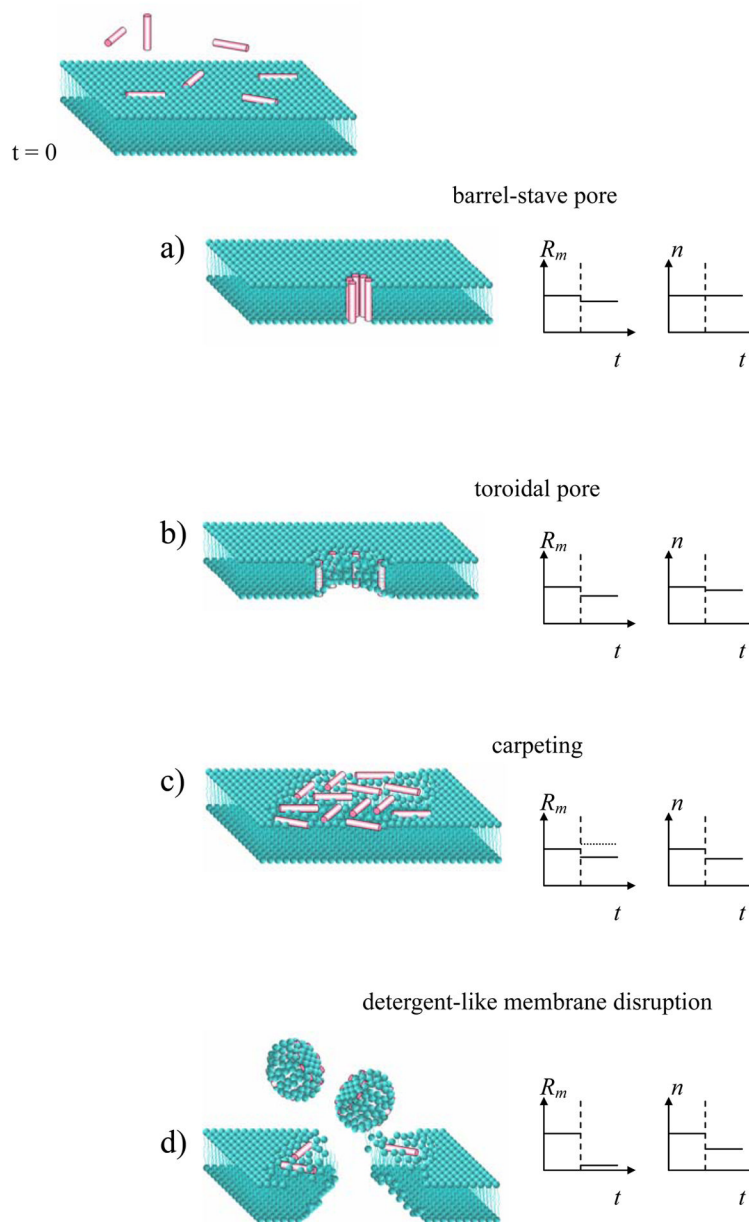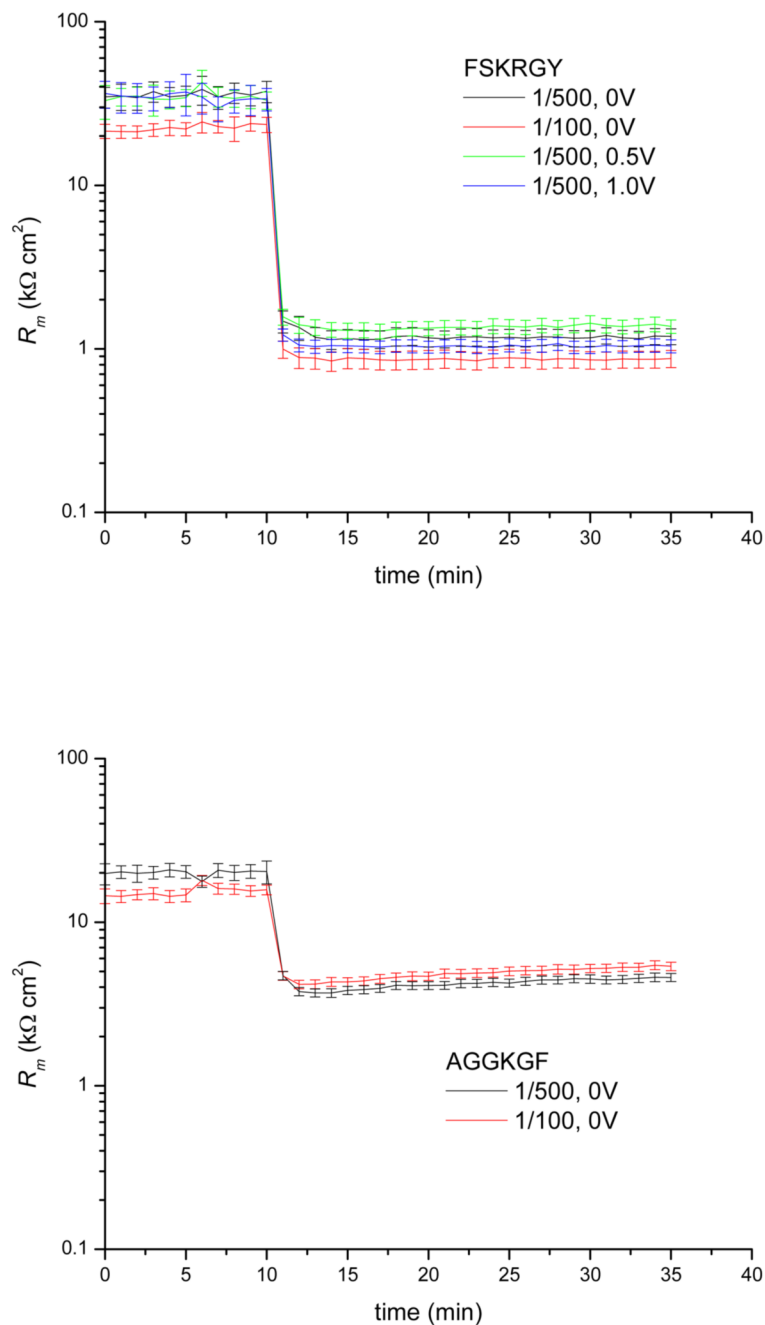
Figure 2.
AMP modes of action and corresponding changes in membrane parameters: resistance R_m and homogeneity n. Vertical dashed line in the graphs shows the moment of peptide injection. If the peptides create a ***barrel-stave pore*** (a), the membrane becomes more permeable to ions (R_m decreases), but the membrane thickness and homogeneity do not change. If the peptides associate in a ***toroidal pore*** (b), the membrane also becomes leakier and the membrane thickness decreases along the pore perimeter resulting in a slightly decreased homogeneity. If the peptides aggregate as in the ***carpet model*** (c), membrane homogeneity certainly decreases while membrane resistance may decrease (in case the peptides introduce a disorder in the lipids) or increase (in case the peptides have opposite, ordering effect [29]). In the ***detergent-like model*** (d) the peptides disrupt the membrane, resulting in a huge decrease or a complete disappearance of membrane resistance. The membrane can still provide an electrochemical barrier if the disrupted regions can be "repaired" by lateral lipid diffusion into those regions.

One may expect a decrease in homogeneity (lower *n*) due to the existence of different membrane regions: intact, disrupted, repaired. Overall, this disruption/repair process would result in a decrease of lipid density and, as a consequence, decrease of membrane resistance R_m, and decrease of membrane thickness (higher C_m).

Figure 3.

Modulus, |Z| and phase angle, Θ, of the electrochemical impedance Z of surface-supported bilayer versus frequency of applied oscillating voltage. DPhPC/PEG2k bilayer (top panel). The measured points (filled circles) were fitted to the response of the electrical circuit shown in Fig. 1 using RC element for the membrane and yielding $R_s = 10$ MΩcm^2, $C_s = 2.1$ μF/cm^2, $R_m = 7.2$ kΩcm^2, $C_m = 0.9$ μF/cm^2, $R_e = 40$ Ωcm^2. Bilayer after the addition of 1/100 P/L AGGKGF peptide (bottom panel). The measured points were fitted using CPE (see Fig. 1) yielding $R_s = 10$ MΩcm^2, $C_s = 2.18$ μF/cm^2, $R_m = 4.9$ kΩcm^2, $Q = 4.35 \times 10^{-6}$/cm^2, $n = 0.84$, $R_e = 42$ Ωcm^2. Note that the units of Q depend on n, see eq.(2). From these values we obtain $C_m = 0.87$ μF/cm^2 at 5 kHz, see eq. (3).

Figure 4.
Resistance of DPhPC/PEG2K bilayer versus time at different peptide/lipid ratios and DC potentials. FSKRGY (top panel) and AGGKGF (bottom panel) was added at t = 10min at the peptide/lipid ratios and DC potentials indicated. The membrane resistance drops within one minute followed by minor equilibration over the next 3–10 minutes. The presence of FSKRGY results in ~5 times lower membrane resistance than the presence of AGGKGF. There is no measurable dependence on membrane potential or peptide concentration (in the range tested).
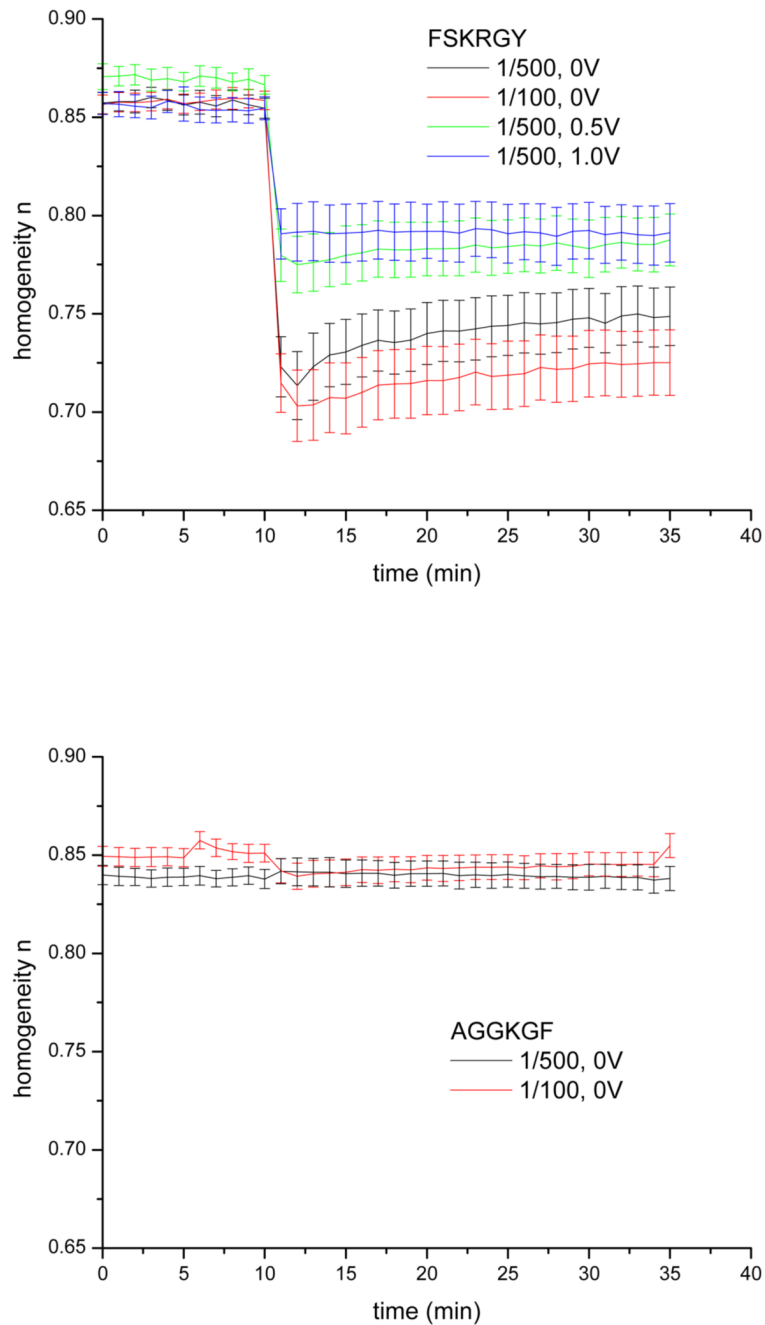
Figure 5.
Membrane homogeneity *n* versus time at different peptide/lipid ratios and DC potentials. FSKRGY (top panel) and AGGKGF (bottom panel) was added at t = 10 min at the peptide/ lipid ratios and DC bias potentials indicated. For all DC bias potentials and peptide concentrations, *n* decreased upon addition of FSKRGY. No such changes were observed upon addition of AGGKGF. In FSKRGY experiments, more positive membrane potentials resulted in more moderate changes; in addition, the changes were larger at higher peptide concentration. Value of *n* reached minimum within 1–2 minutes, followed by a partial relaxation with a time constant of about 8 min.